IEEE Access
Multidisciplinary ⋮ Rapid Review ⋮ Open Access Journal

Received June 11, 2020, accepted June 18, 2020, date of publication June 26, 2020, date of current version July 9, 2020.

Digital Object Identifier 10.1109/ACCESS.2020.3005175

Design of Intelligent Circuit Characteristic Tester for Use in Harsh Environments

XIAONAN ZHAO[1,2], SHUAI DENG[2], AND YANG LI[1,2]
[1]Tianjin Key Laboratory of Wireless Mobile Communications and Power Transmission, Tianjin Normal University, Tianjin 300387, China
[2]College of Electronic and Communication Engineering, Tianjin Normal University, Tianjin 300387, China

Corresponding author: Xiaonan Zhao (xiaonan5875@163.com)

This work was supported in part by the Natural Science Foundation of Tianjin City under Grant 18JCYBJC86400, in part by the Doctor Fund of Tianjin Normal University under Grant 52XB1604, in part by the Natural Science Foundation of Tianjin City under Grant 19JCQNJC01300, in part by the Doctor Fund of Tianjin Normal University under Grant 52XB1905, in part by the Natural Science Foundation of Tianjin City under Grant 18JCQNJC70900, in part by the National Natural Science Foundation of China under Grant 61704122, and in part by the National Natural Science Foundation of China under Grant 61801327.

ABSTRACT This paper designs and makes an intelligent circuit characteristic tester. It is used to measure the characteristics of a specific amplifier circuit, and then to intelligently determine the reasons for the failure or change of the amplifier due to the change of components.The intelligent circuit characteristic tester is driven by a single chip microcomputer (MSP32F103V) to produce a 1 kHz sinusoidal excitation signal. The influence of the output module resistance is eliminated by an impedance matching circuit, and the input is measured. The input resistance, output resistance and magnification of the measured circuit are calculated by designing the peripheral resistance at both ends of the tested circuit. The output signal of the measured circuit is filtered for DC noise and then input to the single chip microcomputer by the AD637 DC conversion module. The amplifier's input and output resistance, magnification and fault analysis results are automatically processed and measured by the E76 module.For the result of circuit test, the tester can automatically and accurately judge and display the reason of circuit change within 2 seconds.

INDEX TERMS Integrated circuits, automatic testing, microcomputers.

I. DESIGN BACKGROUND

Electronic products are based on electronic components and circuits, which are very rich in variety and widely used in daily production and life [1]. They provide convenience to people's lives, but their failures can have serious impacts. If the electronic circuit fails, it will greatly affect the performance and security of electronic products, and even threaten the safety of people's lives and property. In electronic products, the main source of fault comes from the circuit system [2]; if the failure cannot be rectified immediately, it can cause equipment operation to fail, resulting in a greater loss [3]. Therefore, technicians should take effective measures to deal with circuit system failures, such as strengthening detection [4], fault identification and troubleshooting methods to ensure their safe operation and reduce losses [5].

In this study, we design and fabricate an intelligent circuit characteristics tester [6], measure the characteristics of a particular amplifier [7], and then determine the components responsible for amplifier failure or change [8].

The associate editor coordinating the review of this manuscript and approving it for publication was Qilian Liang.

II. DESIGN SCHEME

A. BLOCK DIAGRAM OF THE OVERALL SYSTEM ARCHITECTURE

Figure 1 shows the measured amplifier circuit. The circuit diagram shows the arrangement of the components on the circuit board. Modular components with pins help ensure that each component can be easily replaced. The absolute value of the resistance relative error used in the circuit does not exceed 5%, and the absolute value of the capacitance relative error does not exceed 20%. The transistor model is 9013, and its beta value is between 60 and 300. The output port of the circuit characteristic tester is connected to the amplifier's input end (Ui), and the input port of the circuit characteristic tester is connected to the amplifier's output end (Uo).

The system is composed of a signal source, impedance matching module, measured network, voltage follower and AD637 DC conversion module, and the network to be tested is a transistor amplifier. The scheme generates the sinusoidal

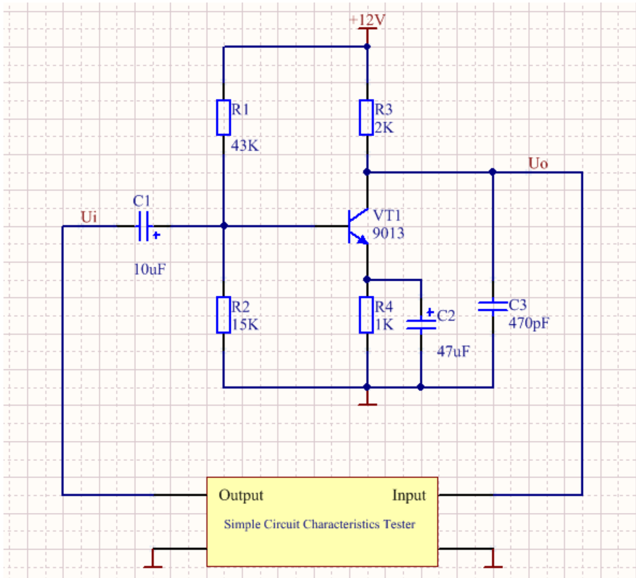

FIGURE 1. Connection diagram of specific amplifier circuit and circuit characteristics tester.

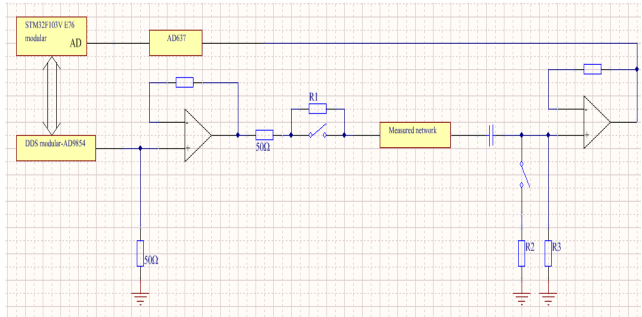

FIGURE 2. System composition.

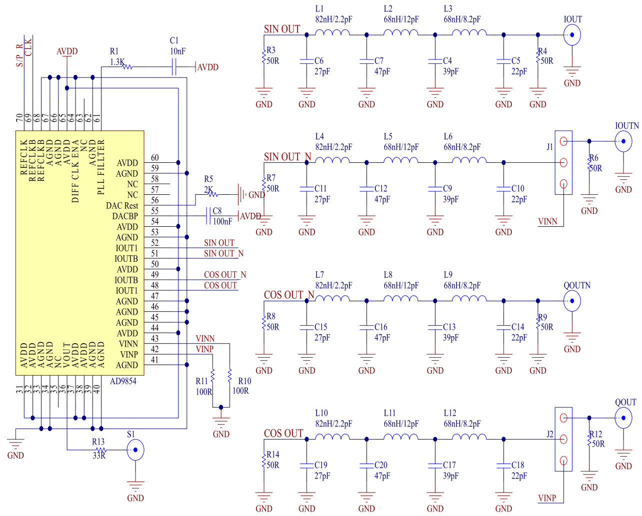

FIGURE 3. AD9854 chip.

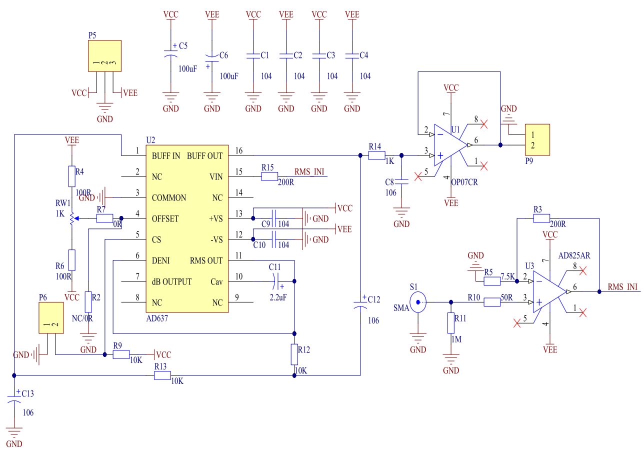

FIGURE 4. AD637 DC conversion module.

signal with adjustable frequency through the single chip STM32F103V drive chip AD9854, eliminates the influence of the signal source output resistance through the impedance matching module, and inputs the signal to the circuit under test. It can obtain the input and output resistances and the magnification of the circuit under test. After the output signal of the measured network is processed by the capacitance voltage follower, it is converted into a DC signal for input to the single chip microcomputer (STM32F103V) by the AD637 DC conversion module. The input resistance, output resistance, circuit magnification and corresponding fault analysis are automatically measured by the debugged E76 module and displayed on the LCD display screen.

B. INTERPRETATION OF HARDWARE CIRCUIT MAIN MODULE DESIGN——SYSTEM

1) FORWARD SIGNAL SOURCE

According to the theoretical analysis, the circuit is designed as follows:

AD9854 chip: Driven by a single chip microcomputer (STM32F103V), the DDS chip (AD9854) produces a stable, frequency-programmable modulated sinusoidal and cosine output when an accurate reference frequency is entered.

2) DC CONVERSION MODULE

The AC voltage is diverted to the single input end of the unipolar current-driven squared divider circuit [9]. The squared divider's output current-driven components and external average capacitance form a low pass filter, which returns the squared or divider after the output current, completes the calculation of the effective value and outputs the converted DC signal [10].

III. CIRCUIT

A. HARDWARE CIRCUIT —— PHYSICAL CONNECTION DIAGRAM

We connect the stm32, Arduino, camera, temperature and humidity sensor, Bluetooth module, infrared emission module, infrared receiving module, player, light intensity sensor and so on of the raspberry pi, integrated nb-iot module, as shown in Figure 4. The integrated system is then centralized inlaid into the "doll" and equipped with a detection function, as shown in Figure 5.

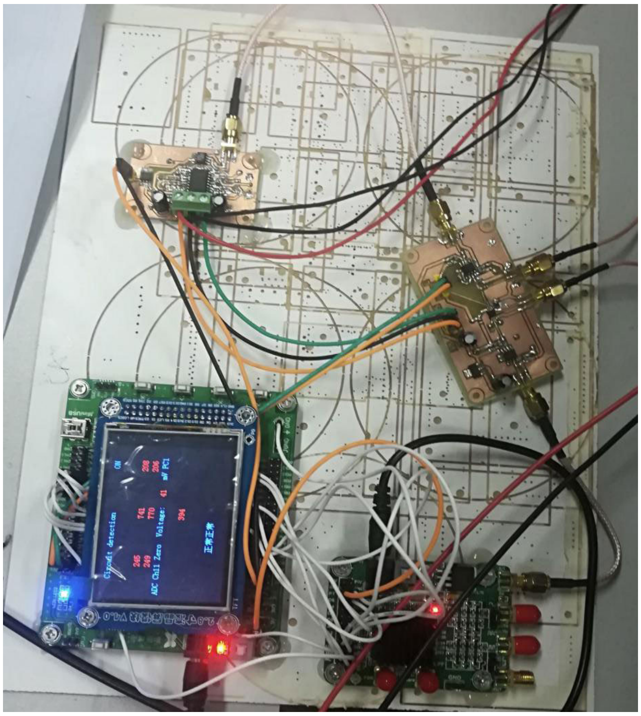

FIGURE 5. Physical connection diagram.

B. PROGRAMMING

The input resistance, output resistance, and gain detection module output the 1 kHz sinusoidal signal input to the circuit under test.

The output step of the amplitude-frequency characteristic detection module is a 1 kHz ~ 200 kHz sweep frequency sine wave signal, which is input to the circuit under test.

The circuit state is obtained by comparing the data items for the 100 Hz, 1 kHz and 1 MHz input states.

C. THEORETICAL ANALYSIS AND CALCULATION OF SYSTEMS

1) SYSTEM PRINCIPLE

Let the resulting sinusoidal signal be, and the amplified signal be $V_I = A\cos\omega t V_o = AK\cos(\omega t + \varphi)$. K represents the magnification and φ represents the magnified phase. After amplification through the effective value detection module, the output, input resistance and gain signals are calculated by the single chip microcomputer.

2) NETWORK ANALYSIS UNDER TEST

The network under test is a single-tube (C9013) amplifier circuit, which is a Q-point stable partial voltage bias circuit, as shown in Figure 7.

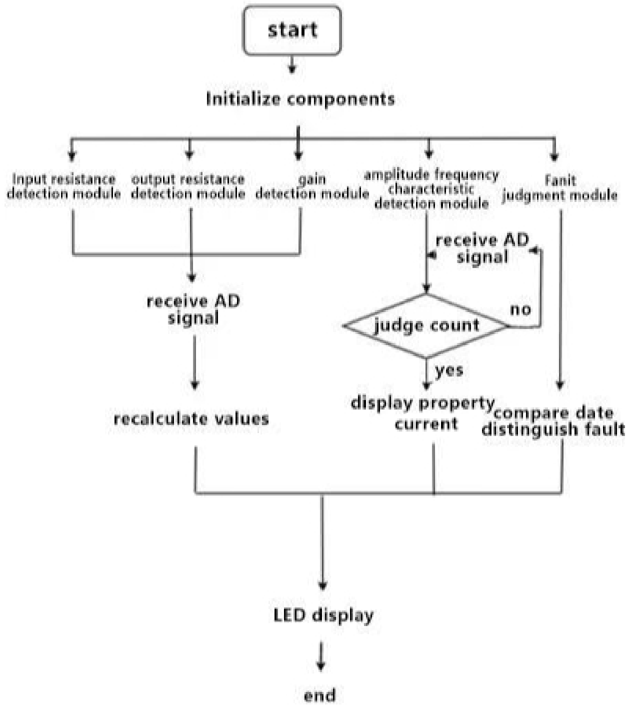

FIGURE 6. Programming.

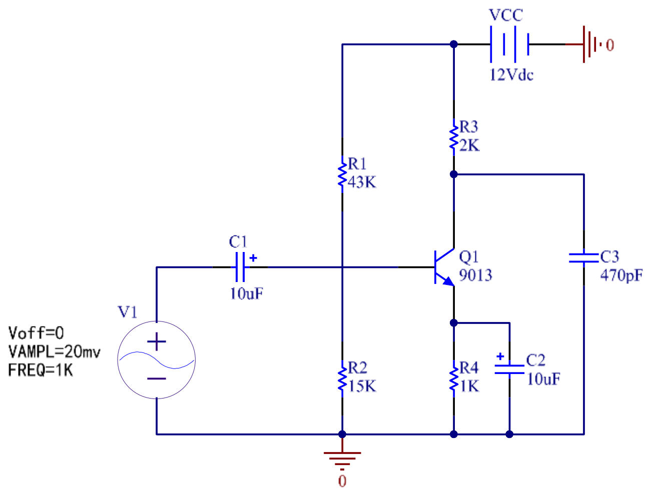

FIGURE 7. Measured circuits.

(1) The measured beta = 172. Using static point analysis:

$$U_b = \frac{R_2}{R_1 + R_2} V_{CC}, \quad I_e = \frac{U_e}{R_4} \; U_e = U_b - U_{beQ},$$
$$I_c \approx I_e, \quad I_B = \frac{I_e}{1+\beta}, \; U_C = V_{CC} - I_C R_3.$$

(2) The theoretical magnification, input resistance and output resistance are given by:

$$r_{be} \approx r_{bb'} + r_{be'} \approx r_{bb'} + (1+\beta)\frac{U_T}{I_e}$$

(26 mV at room temperature),

$$U_T \quad R_i = R_1//R_2//r_{be}, \quad R_0 = R_3\ A_u = \frac{U_o}{U_i} = -\frac{BR_3}{r_{be}}.$$

(3) In the measurement process, any amplifier circuit can be equivalent to a two-terminal network.

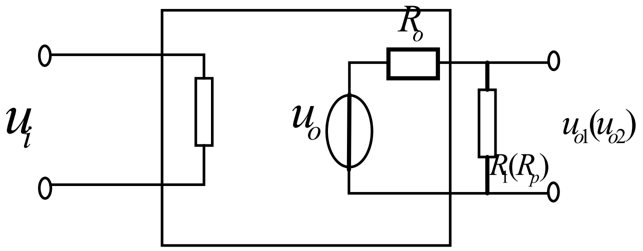

FIGURE 8. Output resistance measurement circuit.

A, R_i and R_o represent the magnification, input resistance, and output resistance, respectively. From Figure 8, the two-port network has:

$$\frac{Au_iR}{R_o + R_1} = u_{o1}\frac{Au_iR_P}{R_o + R_p} = u_{o2}$$

where A, R_i and R_o represent the magnification, input resistance, and output resistance, respectively.

$$R_o = R_1R_2\frac{(u_{o1} - u_{o2})}{u_{o2}(R_1 + R_2) - u_{o1}R_2}$$

$$A = u_{o1}u_{o2}\frac{R_1}{u_i[u_{o2}(R_1 + R_2) - u_{o1}R_2]}$$

From Figure 9,

$$Au_i = u_o \quad Au_i\frac{R_i}{R_s + R_i} = u_o',\ R_i = \frac{u_o'R_s}{Au_i - u_o'}$$

where R_s represents the source resistance value and u_o', a test value.

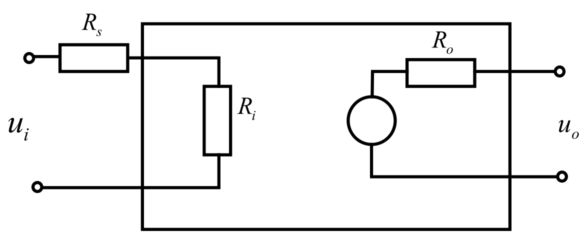

FIGURE 9. Input circuit measurement circuit.

IV. SUMMARY

In this study, we designed a type of intelligent circuit characteristics tester, to reveal circuit problems in a timely fashion, thus improving electronic output. Our design has many shortcomings, and further research is needed to

(1) Supplement this research with more data to further improve the system.

(2) Allow detection of circuit faults beyond short or open RC circuits.

V. RESULTS

Test number	Test target	Test conditions	Test records
(1)	Automatic measurement of input resistance. The absolute value of the relative error does not exceed 10%	Measure and display the amplifier's input resistance	Display input resistance between 0.8k Ω ~3k Ω
		Disconnect B pole	Display input resistance between 11.1k Ω ±1.1k Ω
		Disconnect B pole and then disconnect	Display input resistance between 43k Ω ± 4.3k Ω
		R2	
(2)	Automatic measurement of output resistance. The absolute value of the relative error does not exceed 10%.	Measure and display the amplifier's output resistance	Display output resistance between 2k Ω ± 0.2k Ω
		Replace R3 with 1k Ω resistor	Display output resistance between 1k Ω ± 0.1k Ω
(3)	Automatic measurement of amplifier gain at 1 kHz frequency. The absolute value of the relative error does not exceed 10%.	Measure and display the amplifier's gain at 1 kHz input frequency	Display gain between 100 and 200.
		Use Wire Direct Tester Input and Output End	Show gain between 1±0.1.
(4)	Automatic measurement of the frequency amplitude characteristic curve, showing the frequency upper limit. The absolute value of the relative error does not exceed 20%	Measure and display the amplifier's amplitude characteristic curve, showing the on-line frequency value	Display frequency amplitude characteristic curve
			Show fH = between 169 kHz ±34 kHz
		Change C3 to 1000 pF	Display frequency amplitude characteristic curve
			shows fH between 79.6 kHz ± 16 kHz

（5）	On or off fault determination for R1 - R4	Open R1	Fault Cause Show Correct
		Open R3	Fault Cause Show Correct
		Short Circuit R2	Fault Cause Show Correct
		Short Circuit R4	Fault Cause Show Correct
（6）	Capacitor open circuit fault determination for C1 - C3.	Open Circuit C1	Fault Cause Show Correct
		Open Circuit C2	Fault Cause Show Correct
		Open Circuit C3	Fault Cause Show Correct
（7）	The capacity of one capacitor in C1- C3 is doubled.	Increase C1	Reasons for Change; Show Correct
		Increase C2	Reasons for Change; Show Correct
		Increase C3	Reasons for Change; Show Correct

REFERENCES

[1] B. H. Dobkin and A. Dorsch, "The promise of mHealth: Daily activity monitoring and outcome assessments by wearable sensors," *Neurorehabilitation Neural Repair*, vol. 25, no. 9, pp. 788–798, Nov. 2011.

[2] X. Zhao, J. Li, W. Liu, J. Zhang, and Y. Li, "Design of the sleeping aid system based on face recognition," *Ad Hoc Netw.*, vol. 99, Mar. 2020, Art. no. 102070.

[3] R. Puche-Panadero, J. Martinez-Roman, A. Sapena-Bano, and J. Burriel-Valencia, "Diagnosis of rotor asymmetries faults in induction machines using the rectified stator current," *IEEE Trans. Energy Convers.*, vol. 35, no. 1, pp. 213–221, Mar. 2020.

[4] X. Li, "The single—Tube resistance—Capacitance coupled amplifier simulation based on multisim 10," *J. Luohe Vocational Technol. College*, vol. 12, no. 5, pp. 29–31, Oct. 2013.

[5] D. Thomas *et al.*, "Optimizing power consumption of Wi-Fi for IoT devices: An MSP430 processor and an ESP-03 chip provide a power-efficient solution," *IEEE Consum. Electron. Mag.*, vol. 5, no. 4, pp. 92–100, Oct. 2016.

[6] A. J. Kalb and E. M. Miranda, "Electrical networks and methods of forming the same," U.S. Patent 8 884 646 B2, Nov. 11, 2014.

[7] R. V. Kravchuk, O. A. Katok, V. V. Kharchenko, A. A. Kotlyarenko, and M. P. Rudnyts'kyi, "Determination of the mechanical characteristics of the metal of the equipment of nuclear power stations from hardness measurement and indentation data," *Strength Mater.*, vol. 51, no. 3, pp. 381–387, May 2019.

[8] S. Roy, M. I. Jaeson, Z. Li, S. Mahboob, R. J. Jackson, B. Grubor-Bauk, D. K. Wijesundara, E. J. Gowans, and C. Ranasinghe, "Viral vector and route of administration determine the ILC and DC profiles responsible for downstream vaccine-specific immune outcomes," *Vaccine*, vol. 37, no. 10, pp. 1266–1276, Feb. 2019.

[9] H. J. Bergveld, D. Büthker, C. Castello, T. Doorn, A. de Jong, R. van Otten, and K. de Waal, "Module-level DC/DC conversion for photovoltaic systems: The delta-conversion concept," *IEEE Trans. Power Electron.*, vol. 28, no. 4, pp. 2005–2013, Apr. 2013.

[10] P. Bhatnagar, R. Agrawal, N. Kumar Dewangan, S. K. Jain, and K. Kumar Gupta, "Switched capacitors 9-level module (SC9LM) with reduced device count for multilevel DC to AC power conversion," *IET Electr. Power Appl.*, vol. 13, no. 10, pp. 1544–1552, Oct. 2019.

XIAONAN ZHAO received the Ph.D. degree from Tianjin University, Tianjin, in 2015. He is currently working with the College of Electronic and Communication Engineering, Tianjin Normal University. His research interests include wireless communication channel measurement and modeling.

SHUAI DENG entered the School of Electronics and Communication Engineering, Tianjin Normal University, in 2017. In 2019, he participated in the engineer program and studied communication related majors. His current research interest includes electronic hardware debugging.

YANG LI received the B.E. and M.E. degrees from the College of Information Technology and Science, Nankai University, Tianjin, in 2008 and 2012, respectively, and the Ph.D. degree from the Department of Engineering, Tohoku University, Sendai, in 2017. He is currently with the College of Electronic and Communication Engineering, Tianjin Normal University. His research interests include antenna design, EM-wave propagation, and sensor networks.